

CEP152 is a genome maintenance protein disrupted in Seckel syndrome

Ersan Kalay^{1,2,3}, Gökhan Yigit^{2-4,23}, Yakup Aslan⁵, Karen E Brown⁶, Esther Pohl^{2,3}, Louise S Bicknell⁷, Hülya Kayserili⁸, Yun Li^{2,3}, Beyhan Tüysüz⁹, Gudrun Nürnberg^{3,4,10}, Wieland Kiess¹¹, Manfred Koegl¹², Ingelore Baessmann^{3,10}, Kurtulus Buruk¹³, Bayram Toraman¹, Saadettin Kayipmaz¹⁴, Sibel Kul¹⁵, Mevlit Ikbali¹⁶, Daniel J Turner¹⁷, Martin S Taylor⁷, Jan Aerts¹⁷, Carol Scott¹⁷, Karen Milstein¹⁸, Helene Dollfus¹⁹, Dagmar Wiczorek²⁰, Han G Brunner²¹, Matthew Hurles¹⁷, Andrew P Jackson⁷, Anita Rauch²², Peter Nürnberg^{3,4,10}, Ahmet Karagüzel¹ & Bernd Wollnik²⁻⁴

Functional impairment of DNA damage response pathways leads to increased genomic instability. Here we describe the centrosomal protein CEP152 as a new regulator of genomic integrity and cellular response to DNA damage. Using homozygosity mapping and exome sequencing, we identified *CEP152* mutations in Seckel syndrome and showed that impaired CEP152 function leads to accumulation of genomic defects resulting from replicative stress through enhanced activation of ATM signaling and increased H2AX phosphorylation.

Maintenance of genomic integrity is required for cell survival and function. As the accumulation of DNA damage has an important effect on cell viability, organisms have evolved mechanisms to protect the integrity of DNA by inducing DNA damage responses and cell cycle arrest or by triggering apoptosis¹. Disruption of these mechanisms can lead to increased genomic instability, which is a key factor for the development of cancer and is involved in aging. Two important regulators of DNA-damage responses are the phosphoinositide 3-kinase-related serine/threonine kinases ATM (Ataxia-Telangiectasia Mutated) and ATR

(Ataxia-Telangiectasia and Rad3 related)^{1,2}. Whereas ATM is activated in response to DNA double-strand breaks, ATR is involved mainly in responses to single-stranded DNA induced by ultraviolet light damage or replication arrest. ATM and ATR both trigger an overlapping set of cellular responses that promote cell cycle arrest and DNA repair³.

Recently, it was reported that a hypomorphic *ATR* mutation is associated with embryonic replicative stress, accelerated aging in mice and Seckel syndrome in humans^{4,5}. Seckel syndrome (MIM210600) is a heterogeneous autosomal recessive disorder characterized by a proportionate short stature, severe microcephaly and mental retardation, and a typical 'bird-head' facial appearance⁶. Initially, we clinically evaluated five consanguineous families with Seckel syndrome originating from an isolated rural area in Turkey (**Fig. 1, Supplementary Figs. 1 and 2 and Supplementary Table 1**). We genotyped DNA from four affected members of three families using the 250K SNP Array (Affymetrix) and obtained a single maximum \log_{10} odds (LOD) score of 6.03 for a region between rs1598206 and rs2330591 on chromosome 15q21.1–q21.2 (**Fig. 1b**). Subsequent fine mapping using microsatellite markers confirmed shared homozygosity and a founder haplotype in a 3.4-Mb region between markers *D15S123* and *D15S1017*. This genomic region contains 28 known and predicted genes. Microcephalic osteodysplastic primordial dwarfism type II (MOPDII, MIM210720), which shows overlapping features with Seckel syndrome, was recently associated with mutations in *PCNT*, the centrosomal pericentrin gene^{7,8}. Hence, we considered *CEP152*, the centrosomal protein 152 gene located in the critical region, to be a highly relevant candidate gene.

Sequencing of all 27 exons of *CEP152* (**Supplementary Table 4**) revealed a homozygous splice donor-site mutation in intron 4, c.261+1G>C, which co-segregated with the founder haplotype and the disease in all affected family members (**Supplementary Fig. 3**) and was not found in 250 healthy Turkish control individuals. The c.261+1G>C mutation completely disrupted the splice donor site, as shown through RT-PCR analysis of RNA from affected individuals. We found four different aberrant transcripts likely to cause loss of protein function though partial functional activity of one mutant protein, Val86_Asn87del, could not be excluded (**Supplementary Fig. 4**).

¹Department of Medical Biology, Faculty of Medicine, Karadeniz Technical University, Trabzon, Turkey. ²Institute of Human Genetics, University of Cologne, Cologne, Germany. ³Center for Molecular Medicine Cologne (CMCC), University of Cologne, Cologne, Germany. ⁴Cologne Excellence Cluster on Cellular Stress Responses in Aging-Associated Diseases (CECAD), University of Cologne, Cologne, Germany. ⁵Department of Pediatrics, Faculty of Medicine, Karadeniz Technical University, Trabzon, Turkey. ⁶Chromosome Biology Group, Medical Research Council Clinical Sciences Centre, Imperial College School of Medicine, Hammersmith Hospital, London, UK. ⁷Medical Research Council (MRC) Human Genetics Unit, Institute of Genetics and Molecular Medicine, Western General Hospital, Edinburgh, UK. ⁸Department of Medical Genetics, Istanbul Medical Faculty, Istanbul University, Istanbul, Turkey. ⁹Department of Pediatric Genetics, Cerrahpasa Medical Faculty, Istanbul University, Istanbul, Turkey. ¹⁰Cologne Center for Genomics, University of Cologne, Cologne, Germany. ¹¹Department of Women and Child Health, Hospital for Children and Adolescents, University of Leipzig, Leipzig, Germany. ¹²Preclinical Target Development and Genomics and Proteomics Core Facilities, German Cancer Research Center, Heidelberg, Germany. ¹³Department of Clinical Microbiology, Faculty of Medicine, Karadeniz Technical University, Trabzon, Turkey. ¹⁴Department of Oral Diagnosis and Radiology, Faculty of Dentistry, Karadeniz Technical University, Trabzon, Turkey. ¹⁵Department of Radiology, Faculty of Medicine, Karadeniz Technical University, Trabzon, Turkey. ¹⁶Department of Medical Genetics, Faculty of Medicine, Karadeniz Technical University, Trabzon, Turkey. ¹⁷Wellcome Trust Sanger Institute, Wellcome Trust Genome Campus, Hinxton, Cambridge, UK. ¹⁸Division of Human Genetics, National Health Laboratory Service and The University of Witwatersrand, Johannesburg, South Africa. ¹⁹Centre de Référence pour les Affections Rares Génétiques Ophtalmologique, Service de Génétique Médicale, Hôpitaux Universitaires de Strasbourg, Strasbourg, France. ²⁰Institut für Humangenetik, Universitätsklinikum Essen, Essen, Germany. ²¹Department of Human Genetics, Radboud University Nijmegen Medical Centre, Nijmegen, The Netherlands. ²²Institute of Medical Genetics, Zürich University, Zürich, Switzerland. ²³These authors contributed equally to this work. Correspondence should be addressed to B.W. (bwollnik@uni-koeln.de) or E.K. (ersankalay@hotmail.com).

Received 9 August; accepted 12 November; published online 5 December 2010; doi:10.1038/ng.725

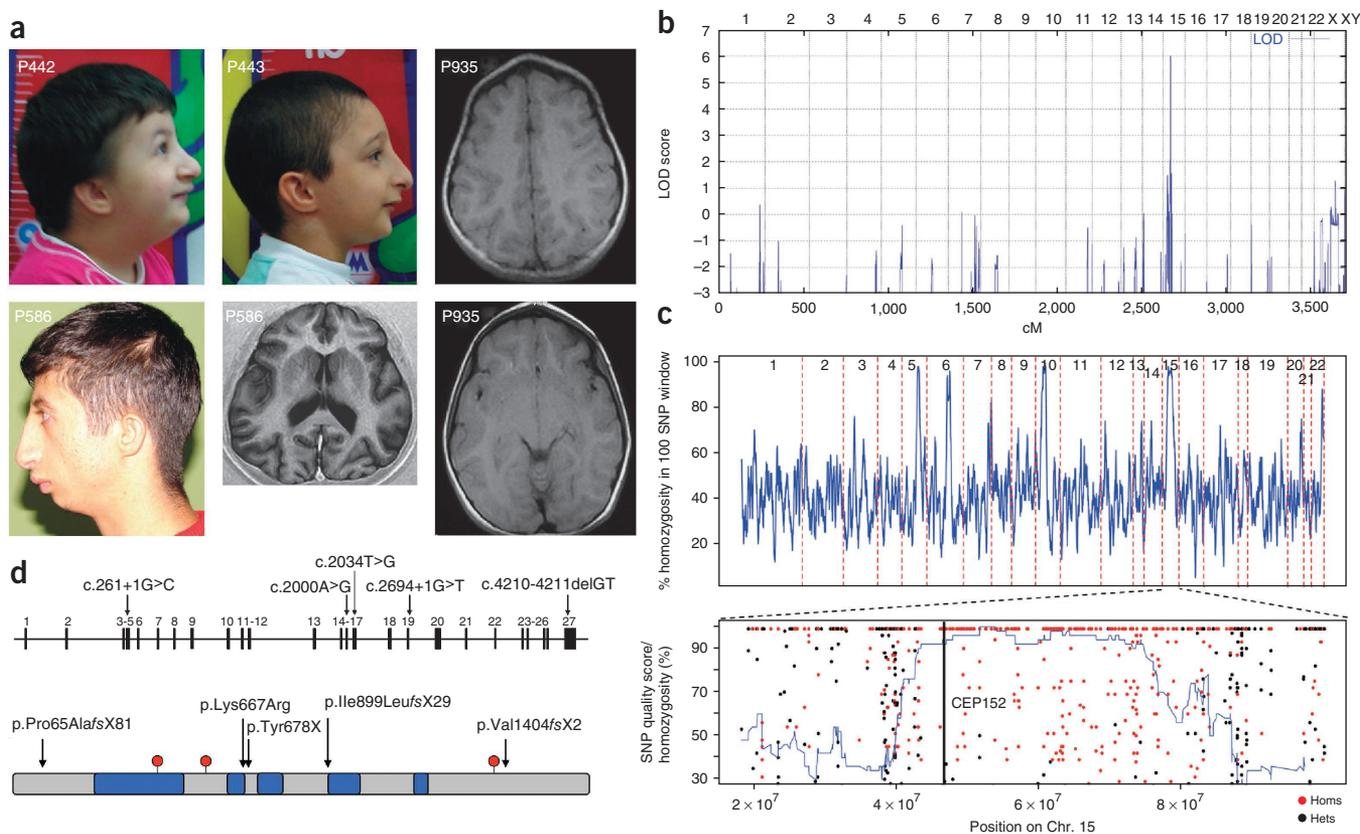


Figure 1 Clinical and molecular characterization of *CEP152* Seckel subjects. **(a)** Clinical characteristics of subjects 442, 443 and 586 presenting with microcephaly, sloping forehead, high nasal bridge, beaked nose and retrognathia. Informed consents to publish the photographs were obtained from the subjects' parents. Cranial magnetic resonance imaging of subjects 586 and 935 showing simplified gyri. **(b)** Genome-wide graphical view of LOD scores using SNP array homozygosity mapping in four affected subjects, 442, 443, 586 and 633, indicated significant linkage to chromosome 15q21.1–q21.2. **(c)** Above, homozygosity (blue line) was measured as the percent of homozygous sites within a sliding window of 100 variant sites, relative to the reference genome, obtained from the exome sequencing data. *CEP152* is located on chromosome 15, which harbors one of the longest stretches of homozygosity in this genome. Below, the chromosomal locations of all single nucleotide variants called on chromosome 15 are plotted against the genotype quality for that variant. Homozygous variants are plotted in red, and heterozygous variants are plotted in black. Homozygosity (blue line) is measured as the fraction of homozygous sites within a sliding window of 50 variant sites (relative to the reference genome) called from the exome sequencing data. **(d)** Above, the genomic structure of human *CEP152*. The position of each mutation is shown on the coding DNA level. Below, the protein structure of *CEP152* with predicted coiled-coil domains (blue boxes) and Thr/Ser-phosphorylation sites (red). The position and the predicted effects of the mutations on *CEP152* are marked by arrows.

Independently, we identified *CEP152* as the causative gene in a French individual with Seckel syndrome of Turkish origin born to consanguineous parents through the use of an exome sequencing strategy (**Supplementary Methods**). We identified seven new and homozygous nonsense and essential splice-site variants that were expected to have a severe impact on gene function (**Supplementary Table 2**). Of these seven variants, a G>C transversion at the +1 position of a donor site was embedded within a ~35-Mb tract of homozygosity on chromosome 15, which was the longest tract of homozygosity observed on any autosome in this individual (**Fig. 1c**). None of the other variants were associated with a large region of homozygosity. This mutation is the same c.261+1G>C Turkish founder mutation in *CEP152* described above. These data demonstrated that mutation identification through exome sequencing, in conjunction with simultaneous analysis of homozygous stretches, can be used as an efficient approach to gene identification in autosomal recessive disorders.

In addition, sequencing *CEP152* in further subjects with Seckel syndrome identified two individuals that were compound heterozygous for likely loss-of-function mutations. One subject of Italian origin

from Germany was compound heterozygous for a nonsense mutation, c.2034T>G (p.Tyr678X), and an intron 19-splice donor-site mutation, c.2694+1G>T, leading to retention of the entire intron 19 in the *CEP152* mRNA (r.2694G_ins3581, Ile899LeufsX29) (**Supplementary Fig. 5**). Because the phenotype of this subject was as severe as the phenotypes seen in the Turkish families, it is likely that the c.261+1G>C Turkish founder mutation has similar functional consequences as the mutation seen here. A subject from South Africa was compound heterozygous for a paternally inherited 2-bp deletion, c.4210–4211delGT (p.Val1404fsX2, exon 27), and a maternally inherited missense mutation, c.2000A>G (exon 15), affecting the highly conserved lysine at position 667 (p.Lys667Arg) (**Fig. 1d** and **Supplementary Fig. 3**). Very recently, mutations in *CEP152* have been associated with microcephaly in an Eastern Canadian subpopulation⁹.

CEP152 encodes a 1,654 amino acid protein that was originally identified in a proteomic screen of human centrosomes¹⁰. Analysis of the subcellular localization of *asl* (*asterless*), the *Drosophila* ortholog of *CEP152*, has shown it to be associated with the periphery of centrioles, where it is involved in the initiation of centriole duplication¹¹. Expression of *CEP152* in HEK293T cells revealed fluorescence

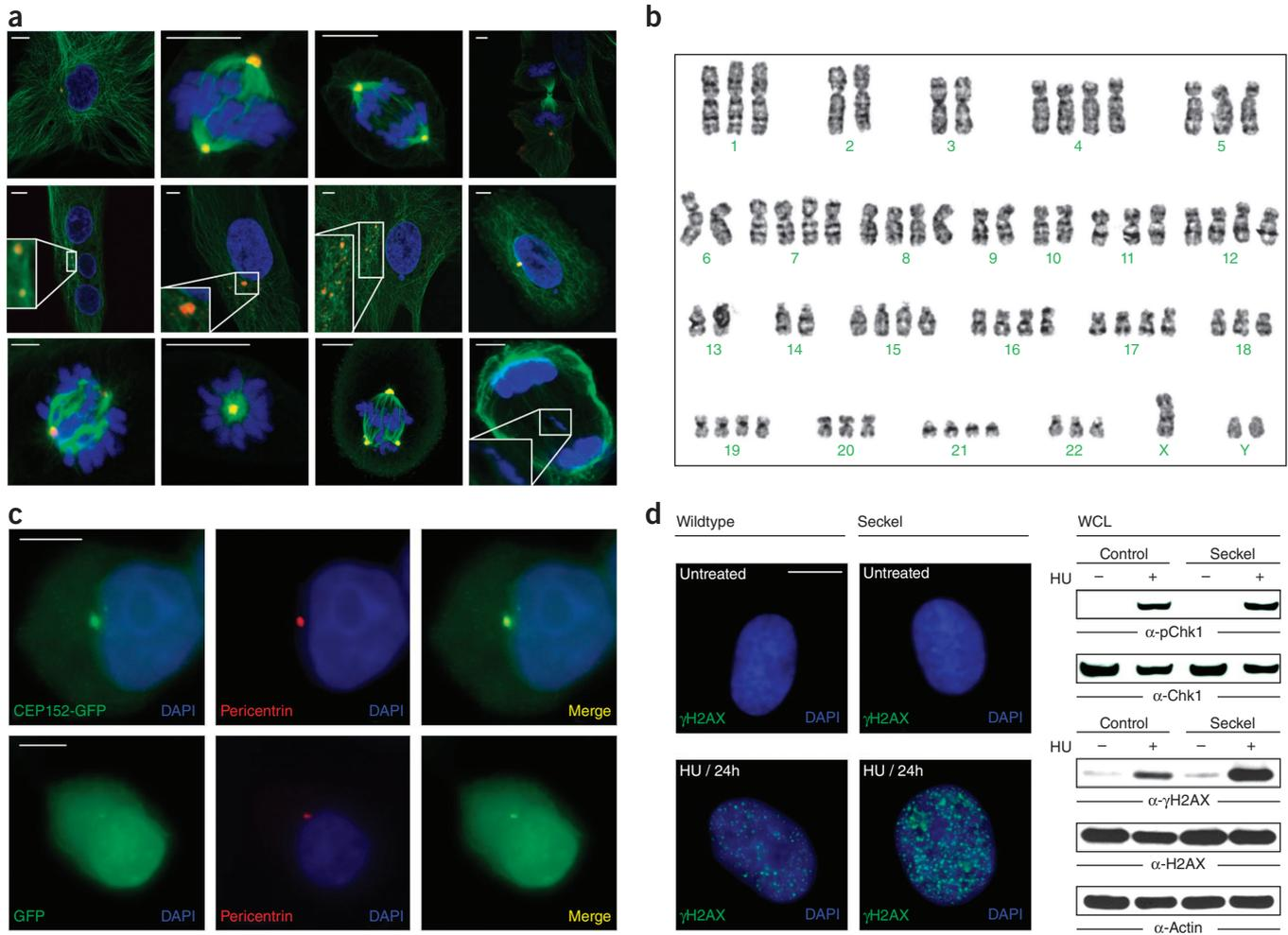


Figure 2 Characterization of *CEP152* Seckel cells. **(a)** Mitotic morphology of *CEP152* Seckel fibroblasts. Immunofluorescence staining of *CEP152* Seckel fibroblasts carrying the c.261+1G>C mutation with antibodies against α -tubulin (green), pericentrin (red) and DAPI staining of DNA (blue). Above, from left to right, control fibroblasts showing normal mitotic morphology of interphase, metaphase, anaphase and telophase. Middle, Seckel interphase cells containing three equally sized nuclei and two centrosomes without astral microtubules (inset, tenfold magnification), two unseparated centrosomes per nucleus without asters (inset, threefold magnification), fragmented centrosomes without asters and micronuclei (inset, twofold magnification), and partially depolymerized microtubules together with micronuclei in addition to a main nucleus. Below, abnormal Seckel metaphases showing incorrectly aligned chromosomes on the metaphase plate, a monopolar spindle with a large centrosome and reduced spindle, a tripolar spindle with differently sized and structurally compromised centrosomes, and an abnormal Seckel telophase showing defects in cytokinesis (inset, twofold magnification). Scale bars, 5 μ m. **(b)** Aneuploid metaphase karyotype of a *CEP152* Seckel lymphocyte. **(c)** Centrosomal localization of wildtype *CEP152* in HEK293T cells expressing either GFP-tagged wildtype *CEP152* (above) or GFP as a control (below). Additional staining was with pericentrin (red) and DAPI (blue). **(d)** DNA-damage response in wildtype and Seckel fibroblasts. H2AX phosphorylation of wildtype and *CEP152* Seckel primary fibroblasts after treatment with hydroxyurea (HU) (left). Protein blot analysis of HU-induced phosphorylation of CHK1 (Ser345) and H2AX (Ser139) (right). Equal protein loading was confirmed by re-probing of the membranes with antibodies against CHK1 or H2AX and actin antibodies.

staining of the centrosomes, where it co-localized with pericentrin (Fig. 2)¹². To determine the functional effect of *CEP152* deficiency on genomic stability, we analyzed the morphology of *CEP152*-deficient Seckel fibroblasts during interphase and during different stages of mitosis. A substantial number of Seckel fibroblasts contained multiple, differently sized nuclei and centrosomes, micronuclei and fragmented centrosomes during interphase (Fig. 2a and Supplementary Fig. 6). Metaphase karyotyping of *CEP152*-deficient Seckel lymphocytes showed aneuploidy in 15 out of a total 109 metaphase spreads (Fig. 2b). During metaphase, we observed incorrectly aligned chromosomes, monopolar spindles with a single large centrosome, triple spindles with differently sized and structurally compromised centrosomes, and prematurely separated sister chromatids in Seckel cells. Statistical analysis revealed that *CEP152* deficiency leads to

an increased number of cells containing multiple nuclei and centrosomes, fragmented centrosomes and an increased frequency of aberrant cell divisions.

Moreover, the number of *CEP152*-deficient cells in telophase was decreased. Most strikingly, *CEP152*-deficient cells appeared to be arrested at early anaphase, reflected by an increased number of early anaphase figures in fixed Seckel populations when compared to the wildtype population (Supplementary Fig. 6f). This block may have resulted from problems with chromatid alignment, uneven pulling forces in the spindle, or activation of a checkpoint that responds to weakly attached or misaligned chromosomes. There did not appear to be additional apoptosis at early anaphase. Taken together, these data clearly showed centrosomal and mitotic aberrations caused by *CEP152* mutations.

In addition, Seckel cells showed an overall increased sensitivity to oxidative stress and responded to this stress with increased apoptosis (Supplementary Fig. 7). Cell cycle analysis in CEP152 knockdown cells using short hairpin RNA suggested that CEP152 deficiency delays S-phase entry. Furthermore, fewer Seckel cells progressed to the G2/M phase and an increased proportion of Seckel cells stayed in G0/G1. These findings suggest altered ATR-mediated checkpoint activity and increased replicative stress in CEP152-deficient cells.

In order to determine possible defects in DNA repair mechanisms, we measured the mitomycin-C-induced sister chromatid exchange frequency. We observed a substantial increase in chromosome instability in CEP152-deficient lymphocytes (Supplementary Table 3). In a yeast two-hybrid (Y2H) screen using an N-terminal deletion construct of CEP152 as bait, the CDK2-interacting protein (CINP) was identified as an interaction partner of CEP152 in three independent hits. We confirmed the CEP152-CINP interaction by using complementary immunoprecipitation approaches, and we showed that CEP152 constitutively binds to CINP (Supplementary Fig. 8). We observed a weak nuclear staining for both CEP152 and CINP (data not shown). CINP has recently been identified as a genome maintenance protein¹³ that interacts with the ATR-interacting protein (ATRIP) and has an important function in ATR-mediated checkpoint signaling. Silencing of CINP causes increased γ H2AX foci formation, suggesting that CINP contributes to the formation of a functional unit in DNA damage response. The identification of CEP152 as a binding partner of CINP provides additional evidence for an important role of CEP152 in DNA-damage response and genome maintenance.

ATR-mediated phosphorylation of CHK1 and H2AX are the initial steps in response to DNA damage and increased replicative stress^{14,15}. We did not observe a detectable alteration in hydroxyurea-induced phosphorylation of CHK1 in CEP152-deficient cells (Fig. 2d). However, we found that replicative stress leads to enhanced CHK2 phosphorylation in Seckel cells (Supplementary Fig. 8), indicating an increased activation of ATM signaling pathways. Furthermore, we found that formation of hydroxyurea-induced γ H2AX foci in CEP152-deficient cells was increased. Protein blot analysis confirmed that the levels of γ H2AX were considerably higher in hydroxyurea-treated CEP152-deficient cells as compared to wildtype cells. There are likely to be additional mechanisms by which CEP152 might affect ATR checkpoint control and subsequently lead to increased replicative stress, which causes a compensatory activation of CHK2 and γ H2AX. Recent analysis of H2AX phosphorylation in the ATR^{s/s} Seckel mouse model indicated that γ H2AX has been substantially increased throughout embryonic development, particularly in tissues with a high mitotic index⁵. In agreement with our results, a previous study suggested that accumulated replicative stress can activate ATM-dependent DNA damage response and thereby lead to increased H2AX phosphorylation⁵.

In conclusion, we identified the centrosomal protein CEP152 as a new protein involved in the maintenance of genomic integrity and in

the ability to respond to DNA damage. Impaired CEP152 function leads to genomic instability and increased H2AX phosphorylation, a measure of accumulated replicative stress. Our data further support the essential link between genomic instability, as seen in individuals with Seckel syndrome, and the activation of histone H2AX as response to increased replicative stress.

Accession codes. The CEP152 reference sequence is deposited in the NCBI nucleotide database under the accession code NM_014985.2.

Note: Supplementary information is available on the Nature Genetics website.

ACKNOWLEDGMENTS

We thank all family members who participated in this study, E. Milz, A. Alver and A. Coffey for excellent technical assistance, F. Kokocinski and A. Palotie for experimental design, and C. Kubisch, B. Wirth and K. Boss for critical reading of the manuscript. The CINP antibody was a kind gift from D. Cortez (Nashville, Tennessee, USA). This work was supported by the German Federal Ministry of Education and Research (BMBF) by grant numbers 01GM0880 (SKELNET) and 01GM0801 (E-RARE network CRANIRARE) to B.W., the Karadeniz Technical University Research Fund by grant numbers 2008.114.001.02 and 2008.114.001.12 to E.K., the Medical Research Council and Lister Institute to A.P.J. and by the Wellcome Trust, grant 077014/Z/05/Z.

AUTHOR CONTRIBUTIONS

The project was conceived and the experiments were planned by E.K. and B.W. We would like to note that Y.A. and K.E.B. had a comparable contribution to this study. The review of phenotypes and the sample collection were performed by B.W., E.K., Y.A., A.P.J., H.K., B. Tüysüz, W.K., B. Toraman., S. Kayipmaz, S. Kul, M.I., K.M., H.D., D.W., H.G.B. and A.R. Experiments were performed by E.K., G.Y., K.E.B., E.P., L.S.B., Y.L., M.K., I.B., K.B., D.J.T. and C.S. Data analysis was performed by B.W., E.K., G.N., P.N., A.K., J.A., M.S.T., M.H. and A.P.J. The manuscript was written by B.W., G.Y., E.K. and K.E.B. All aspects of the study were supervised by B.W.

COMPETING FINANCIAL INTERESTS

The authors declare no competing financial interests.

Published online at <http://www.nature.com/naturegenetics/>.

Reprints and permissions information is available online at <http://npg.nature.com/reprintsandpermissions/>.

- Nyberg, K.A., Michelson, R.J., Putnam, C.W. & Weinert, T.A. *Annu. Rev. Genet.* **36**, 617–656 (2002).
- Cimprich, K.A. & Cortez, D. *Nat. Rev. Mol. Cell Biol.* **9**, 616–627 (2008).
- Bonner, W.M. *et al. Nat. Rev. Cancer* **8**, 957–967 (2008).
- O'Driscoll, M., Ruiz-Perez, V.L., Woods, C.G., Jeggo, P.A. & Goodship, J.A. *Nat. Genet.* **33**, 497–501 (2003).
- Murga, M. *et al. Nat. Genet.* **41**, 891–898 (2009).
- Majewski, F. & Goecke, T. *Am. J. Med. Genet.* **12**, 7–21 (1982).
- Rauch, A. *et al. Science* **319**, 816–819 (2008).
- Griffith, E. *et al. Nat. Genet.* **40**, 232–236 (2008).
- Guernsey, D.L. *et al. Am. J. Hum. Genet.* **87**, 40–51 (2010).
- Andersen, J.S. *et al. Nature* **426**, 570–574 (2003).
- Blachon, S. *et al. Genetics* **180**, 2081–2094 (2008).
- Doxsey, S.J., Stein, P., Evans, L., Calarco, P.D. & Kirschner, M. *Cell* **76**, 639–650 (1994).
- Lovejoy, C.A. *et al. Proc. Natl. Acad. Sci. USA* **106**, 19304–19309 (2009).
- Liu, Q. *et al. Genes Dev.* **70**, 1448–1459 (2000).
- Marti, T.M., Hefner, E., Feeney, L., Natale, V. & Cleaver, J.E. *Proc. Natl. Acad. Sci. USA* **103**, 9891–9896 (2006).